Math. Model. Nat. Phenom.
Vol. 8, No. 6, 2013, pp. 165–185
DOI: 10.1051/mmnp/20138611

Resource Competition: A Bifurcation Theory Approach

B.W. Kooi[1] *, P.S. Dutta[2,3], U. Feudel[2]

[1] Department of Theoretical Biology, VU University
de Boelelaan 1085, 1081 HV Amsterdam, The Netherlands

[2] Theoretical Physics/Complex Systems, ICBM
Carl von Ossietzky Universität, PF 2503, 26111 Oldenburg, Germany

[3] Department of Mathematics, Indian Institute of Technology Ropar
Rupnagar-140001, Punjab, India

Abstract. We develop a framework for analysing the outcome of resource competition based on bifurcation theory. We elaborate our methodology by readdressing the problem of competition of two species for two resources in a chemostat environment. In the case of perfect-essential resources it has been extensively discussed using Tilman's representation of resource quarter plane plots. Our mathematically rigorous analysis yields bifurcation diagrams with a striking similarity to Tilman's method including the interpretation of the consumption vector and the resource supply vector. However, our approach is not restricted to a particular class of models but also works with other trophic interaction formulations. This is illustrated by the analysis of a model considering interactively-essential or complementary resources instead of prefect-essential resources. Additionally, our approach can also be used for other ecosystem compositions: multiple resources–multiple species communities with equilibrium or oscillatory dynamics. Hence, it gives not only a new interpretation of Tilman's graphical approach, but it constitutes an extension of competition analyses to communities with many species as well as non-equilibrium dynamics.

Keywords and phrases: bifurcation analysis, competitive exclusion, complementary resources, resource competition, resource quarter plane plot

Mathematics Subject Classification: 34C23, 92D40, 92D25

1. Introduction

Competition among different species is important in many fundamental ecological principles like the *Competitive Exclusion Principle* [6,10], the *Paradox of Plankton* [14], the *Resource-Ratio Theory* [29,30] and the *Resource-Ratio hypothesis of succession* [32]. Competition is also a crucial aspect of the assembly of ecological communities [22] and the adaptive dynamics approach in evolution [7,23].

Most organisms in nature, like bacteria, plants and animal cells, cannot obtain the materials and available energy that they need for growth by taking up a single chemical substance (nutrient) in case

*Corresponding author. E-mail: bob.kooi@vu.nl

of heterotrophs and for autotrophs together with light, from their environment. Instead, a number of different substances must be consumed by the organisms to be able to grow and only when these resources are available in sufficiently high amounts the species can survive. Therefore it is interesting to study growth of species consuming multiple so called essential resources. These are sources (for instance prey, organic matter or nutrient) containing the different essential substances which are considered to be metabolically independent requirements for growth. Examples are a carbon source and a nitrogen source for a bacterium, light and carbon for an alga, or silica and phosphorus for a diatom. In this paper we study competition between two species for two essential resources in a chemostat environment.

The classical mathematical model of two species competing for two resources is the Monod/Liebig chemostat model. In this model the growth of the species feeding on two essential resources is determined by the most limiting resource according to Liebig's minimum law, in which each growth rate is modeled as a Holling type–II functional response. Generally there is no growth limitation by both the resources simultaneously in the Monod/Liebig chemostat model. Only under specific environmental conditions there is co-limitation where both resources limit the growth simultaneously. In this setting the essential resources are called *perfect-essential* and the model is usually concerned with primary producers. For experimental and verification issues we refer to [21, 25, 34] and the references therein. In [21] also an illuminating history of the so-called "resource-ratio theory" is given.

The well-known approach to analyse resource competition is the graphical approach developed by Tilman in [8, 29–31], later extended in [12, 13]. We refer to [12, 27] (and references therein) for an overview of mathematical analysis approaches. In Tilman's graphical approach the resource quarter plane plot is used to analyse the outcome of the competition depending on the model parameters and the resource supply rates. The outcomes of competition are well-known: competitive exclusion where one of the species wins, stable coexistence of both the species or bistability, i.e. each of the species may win depending on the initial conditions.

In this paper we present an alternative analytical method based on bifurcation theory [1, 9, 16, 20]. To elaborate our methodology we analyse again the Monod/Liebig chemostat model with competition of two species for two perfect-essential resources. The analytical results are also supported by numerical bifurcation analysis. Our mathematical method complements the graphical method of Tilman [29, 30] and is more general in the sense that it can be applied to other models with different trophic interactions as well as multiple resources–multiple species models. Additionally it can incorporate non-equilibrium dynamics.

In order to illustrate the proposed method we analyse a chemostat model of competition between two species for two *interactively-essential* resources (i.e. both resources have interactive effects on species growth, hence co-limitation) instead of perfect-essential resources (i.e. a single limiting resource determines the growth of a species). Competition models using the interactively-essential resources can also be used for modelling growth of herbivores (see [26]) besides primary producers.

The corresponding functional response for interactively-essential resources was formulated in [24] (there called the Poisson Arrival Time model) using waiting time theory and in [18] (there called model for complementary resources which are processed in parallel) by modeling uptake and binding processes like in biochemistry. The simplified version of the latter model used here was described and used in a mass-balance model for food webs in [17, 26]. Here we show that in the considered model with interactively-essential resources the outcomes of the competition are the same as in the case for perfect-essential resources: competitive exclusion where one of the species wins, stable coexistence of both the species or bistability, i.e. each of the species may win depending on the initial conditions. However, the dependency on the model parameters and the resource supply rates differ (the resource-dependent growth isoclines have a round corner instead of a right-angle corner).

Finally this considered example illustrates that the bifurcation analysis approach can be used also for similar competition models with different types of ingestion and growth rates. But also for ecosystems with different resources and species compositions or different interplay with the environment.

2. The formulation of the models

To explain our methodology we first analyse a model which has been extensively studied in the literature. In this way we demonstrate that our rigorous mathematical approach can also yield the known results for well studied models. Now we recall the model of competition between two species for two resources in a continuous flow system. Let P_j denote the density of species $j = 1, 2$, and let N_i denote the density of resource $i = 1, 2$ (see Table 1 for a list of symbols). Then the model, sometimes referred to as the

TABLE 1. List of symbols, where resources: $i = 1, 2$ and species: $j = 1, 2$.

Symbol	Meaning
N_i	Resource density
P_j	Species density
D	Dilution rate
N_{ri}	Resource density in inflow
I_{ij}	Maximum ingestion rate
μ_{ij}	Maximum growth rate
f_j	Scaled functional response
K_{ij}	Half-saturation constant
Y	Yield coefficient
m_j	Maintenance rate
TC_j	Transcritical bifurcation parameter value where P_j invades the N_1 and N_2 system
TC_{ij}	Transcritical bifurcation parameter value at which the equilibrium with $P_i = 0$ and $P_j > 0$ looses stability
Z	Double transcritical bifurcation where TC_{12} and TC_{21} coincide

Monod/Liebig model, described and analysed in [29, 30] reads:

$$\frac{dN_i}{dt} = (N_{ri} - N_i)D - \sum_{j=1}^{2} \frac{P_j}{Y_{ij}} \min\left(\frac{r_1 N_1}{K_{1j} + N_1}, \frac{r_2 N_2}{K_{2j} + N_2}\right), \quad i = 1, 2, \tag{2.1a}$$

$$\frac{dP_j}{dt} = P_j\left(\min\left(\frac{r_1 N_1}{K_{1j} + N_1}, \frac{r_2 N_2}{K_{2j} + N_2}\right) - D\right), \quad j = 1, 2, \tag{2.1b}$$

where N_{ri} is the supply density of resource i; r_j is the maximal growth rate of species j; K_{ij} is the half saturation constant (that is, the resource density at which the growth rate is half of its maximum) and Y_{ij} is the yield coefficient (density of species produced per unit of resource density) for species j consuming resource i. All constituents are washed out at fixed dilution rate D.

To compare this model later with a more complex model with co-limitation we analyse a mass-balance version of the same competition system described by the following equations:

$$\frac{dN_1}{dt} = (N_{r1} - N_1)D - I_{11} f_1 P_1 - I_{12} f_2 P_2, \tag{2.2a}$$

$$\frac{dN_2}{dt} = (N_{r2} - N_2)D - I_{21} f_1 P_1 - I_{22} f_2 P_2, \tag{2.2b}$$

$$\frac{dP_1}{dt} = \big(Y(I_{11} + I_{21})f_1 - D - m_1\big)P_1, \tag{2.2c}$$

$$\frac{dP_2}{dt} = \big(Y(I_{12} + I_{22})f_2 - D - m_2\big)P_2, \tag{2.2d}$$

where I_{ij} is the maximum ingestion rate of resource i for species j; $f_j(N_1, N_2)$ is the functional response rate of species j on both the resources i and m_j is the maintenance rate of species j which makes the

model formulation slightly more general. For the sake of simplicity but without loss of generality, we assume that the yield coefficient for all four species/resource interactions are equal and denoted by Y and therefore the growth rate and the ingestion rates are proportional [12] given by $\mu_{ij} = YI_{ij}$ for resources $i = 1, 2$ and species $j = 1, 2$.

Two expressions for the functional response f_j will be considered. When Liebig's minimum law is used like in Eq. (2.1) the two resources are perfect-essential, then the functional responses f_j are determined by:

$$f_j^{min}(N_1, N_2) = \min\Big(\frac{N_1}{K_{1j} + N_1}, \frac{N_2}{K_{2j} + N_2}\Big), \quad j = 1, 2\ . \tag{2.3}$$

Substitution of Eq. (2.3) into Eqs. (2.2) gives a model that is for primary producers equivalent to the Monod/Liebig model for resource competition studied in [8, 12, 13, 29, 30] and in many other papers.

It is important to note that the hyperbolic Holling type–II expressions in the arguments of the minimum operator in Eq. (2.3), are not multiplied by the maximum growth rates, as done in the Monod/Liebig competition model given by Eqs. (2.1). Furthermore, in Eqs. (2.2c) and (2.2d), which describe the species dynamics, the sum of the two growth rates of the species for both resources is taken.

The reasons for the different formulation are as follows. We assume that the resources may also be organisms consumed by the species and that the chemical composition of the resources as well as the species is fixed but they may differ. Eqs. (2.2a) and (2.2b) show that species 1 feeds on both resources with fluxes $I_{11}f_1P_1$ and $I_{21}f_1P_1$ and therefore the quotient of these fluxes equals I_{11}/I_{21} and it is constant. The same holds for species 2 where the quotient I_{12}/I_{22} is constant.

Eqs. (2.2c) and (2.2d) show how the two ingested resources are converted into the species biomass. Both ingested resources are assimilated by each species, and their assimilates are used for growth and maintenance. The quotients of the growth rate and the ingestion rate, the yield, are constant and they are given by $Y = \mu_{ij}/I_{ij}$ for resources $i = 1, 2$ and species $j = 1, 2$. Hence the growth flux of species 1 equals a fixed part of the sum of the two consumption fluxes, that is $YI_{11}f_1P_1$ and $YI_{21}f_1P_1$ with similar expressions for the growth flux of species 2. Since for each species the quotient of these fluxes are constant, the possibly different, chemical compositions of both species remain also constant.

These considerations concerning mass balance, motivated us to use the scaled functional response $f_j^{min}(N_1, N_2)$ Eq. (2.3) in the expressions for the ingestion and growth fluxes multiplied by their maximum values I_{ij} and μ_{ij} respectively. The maximum ingestion rate of species j on resource i, I_{ij}, is obtained when the other resource $3 - i$ is abundant (and therefore resource i is limiting) and where its scaled functional response becomes one: $f_j|_{N_i\to\infty} = N_i/(K_{ij} + N_i)|_{N_i\to\infty} = 1$.

Observe that the uptake process of the resources, including searching and handling, is distinguished from the assimilation, growth and maintenance processes. In other words in the model the stoichiometry's of the resources and the species are different but fixed and constant, and consequently also the chemical composition of the assimilation and maintenance products.

This model formulation holds for both heterotrophic species as well as for primary consumers. Heterotrophic species generally obtain nutrients as packages of complex molecules in biotic compounds. Essential dietary biochemical compounds are for instance vitamins, amino acids and others, see [26] where the identification of potentially limiting nutrients and the understanding of the consequences of nutrient deficiencies is mention the major challenge of ecological research. Since all components of the model are biotic a preferred unit could be C-mols or just biomass.

Primary producers (plants and algae), acquire essential nutrients mostly as single low-molecular compounds, often even abiotic elemental nutrients such as inorganic carbon (DIC), inorganic nitrogen (DIN), phosphorus (DIP) and also light, see also [19]. Since no biomass is directly related to light this nutrient does not add to the growth rate by a separate term. The dynamics of the light intensity is not described by an additional ODE and terms the minimum operator Eq. (2.3), are multiplied by the maximum growth rate, as done in the Monod/Liebig competition model given by Eqs. (2.1). The unit for inorganic nitrogen as a resource is N-mols. Then the chemical coefficient of nitrogen in the species or the fixed C:N ratio, is used to convert the units of the resource fluxes into C-mols.

We consider also the following smooth analog when the two resources are interactively-essential or complementary:

$$f_j^{com}(N_1, N_2) = \frac{N_1/K_{1j}\ N_2/K_{2j}}{N_1/K_{1j} + N_2/K_{2j} - \frac{N_1/K_{1j}\ N_2/K_{2j}}{N_1/K_{1j}+N_2/K_{2j}}}\ ,\ j = 1, 2\ . \tag{2.4}$$

This expression is a simplified version of those derived in [18, 24] and has also been used in [17].

We refer to the model described by Eqs. (2.2) as perfect-essential resources (*PER-model*) when Eq. (2.3) is substituted and as the interactively-essential or complementary resources (*COM-model*) when Eq. (2.4) is substituted. For the COM-model the parameter have the same meaning as in the PER-model and we take the same parameter values given in Table 2. Then the numerical behaviour for small uptake rates is very similar to those of the Liebig's minimum formulation, but the COM-model formulation avoids sharp switches in the PER-model [19]. At these switching points the two growth rate terms in the minimum operator of Liebig's minimum formulation are equal and there is co-limitation. This feature hampers a correct mass balance modeling. In the COM-model there is always co-limitation due to the formulation of the growth rate as the sum of two separate terms related to the two resources (see Eqs. (2.2c), (2.2d) and Eq. (2.4).

Since the resources and the species are expressed in the same dimension/unit the yield coefficient is dimensionless and less than one to avoid spontaneous mass generation. The biomass density of the resource densities and species densities are all given in $\mathrm{mg\,dm^{-3}}$ with parameter values given in Table 2 after [3] for a microbial food chain.

TABLE 2. Parameter set for a microbial food chain model. The ranges for the control parameters are $D = 0.05\ \mathrm{h^{-1}}$ and $0 < N_{ri} \leq 10\ \mathrm{mg\,dm^{-3}}$, $i = 1, 2$. All yield coefficients are the same and denoted by $Y = 0.4$ for all i, j. We take $\epsilon = 0,\ \pm 0.4$.

Parameters	Units		Values			
		Resources	$i=1$	$i=1$	$i=2$	$i=2$
		Species	$j=1$	$j=2$	$j=1$	$j=2$
μ_{ij}	$\mathrm{h^{-1}}$		0.5	0.42	$0.5+0.4\epsilon$	0.42
I_{ij}	$\mathrm{h^{-1}}$		1.25	1.05	$1.25+\epsilon$	1.05
Y	—		0.4	0.4	0.4	0.4
K_{ij}	$\mathrm{mg\,dm^{-3}}$		8	11	16	5.5
m_j	$\mathrm{h^{-1}}$				0.025	

3. Model analysis

In this section we first present a short summary of the graphical method based on resource quarter plane analysis developed by Tilman [30, 31] for the PER-model. Thereafter we present an alternative method based on bifurcation analysis to obtain similar results. We illustrate the alternative method by analysing the model (2.2) for two different resources given by Eq. (2.3)(perfect essential resources) and Eq. (2.4)(complementary resources), respectively.

3.1. Resource quarter plane analysis

We give the plots with parameter values given in Table 2, first for the one species—two resources case and thereafter for the two species—two resources case.

3.1.1. One species—two resources

To construct a three dimensional system (one species—two resources) from model (2.2) we do not need to consider either Eq. (2.2c) or Eq. (2.2d) and in the Eqs. (2.2a) and (2.2b) the associated consumption term. The resource quarter plane plots for the two species PER-model are separately shown in Fig. 1 varying the two parameters N_{r1} and N_{r2} which are the resource density in the inflow and the two state variables N_1 and N_2 which are the densities of the ambient resources. Both quantities, the ambient resource densities N_j and the inflow resource densities N_{rj} have the same dimension/unit and therefore there is only one scale on each axis.

For each species j separately, the zero-growth isocline is formed by horizontal and vertical branches meeting at right angles. In each plot there are two attractors, either E_0 or E_j, were $j = 1$ in Fig. 1**a** or $j = 2$ in Fig. 1**b**. In the region E_0 no species can persist ($P_1 = 0$ and $P_2 = 0$), and in the regions E_j only species j exists ($P_j > 0$ and $P_{3-j} = 0$). The curves are the zero net growth isocline (ZNGI)-curve where the expression between the brackets in Eq. (2.2c) and (2.2d) are zero. In Fig. 1**a** on the vertical branch where $N_{r1} = N^\circ_{11}$, the density of resource 1, N_1, is independent of the inflow of resource 2, N_{r2}.

Using Eq. (2.2c) and (2.2d), the expressions for zero-growth isoclines are

$$Y(I_{1j} + I_{2j})f^\circ_j = D + m_j \ , \quad j = 1, 2 \ , \tag{3.1}$$

where the functional responses $f^\circ_j = f^{min}_j(N^\circ_{1j}, N^\circ_{2j})$, are given by the expressions

$$f^\circ_j = \min\left(\frac{N^\circ_{1j}}{K_{1j} + N^\circ_{1j}}, \frac{N^\circ_{2j}}{K_{2j} + N^\circ_{2j}}\right) = \frac{D + m_j}{Y(I_{1j} + I_{2j})} \quad \text{for } \ j = 1, 2 \ . \tag{3.2}$$

Hence, the Eqs. (3.2) for $j = 1, 2$ are independent, one for each of the species j.

For species j the horizontal and vertical branches are indicated by the resource densities N°_{2j} and N°_{1j} called *subsistence resource concentrations* in [12] and given by

$$N^\circ_{ij} = \frac{(D + m_j)K_{ij}}{Y(I_{1j} + I_{2j}) - (D + m_j)} \ , \tag{3.3}$$

for resources $i = 1, 2$.

At each of the two right-angle corners in Figs. 1**a,b** the Holling type–II functional responses $f_j = f^{min}_j$, $j = 1, 2$ respectively, for both resources $i = 1, 2$ are equal and we have co-limitation. In those points we have

$$f^{min}_j = \frac{N_1}{K_{1j} + N_1} = \frac{N_2}{K_{2j} + N_2}, \tag{3.4}$$

that gives

$$N_2 = \frac{K_{2j}}{K_{1j}} N_1, \tag{3.5}$$

which is a straight line through the origin with slope K_{2j}/K_{1j}. This curve is sometimes called the *switching curve* (see [2]). For $j = 1$ at the right-angle corner in Fig.1**a** we have $N_1 = N^\circ_{11}$ and $N_2 = N^\circ_{21}$, which implies

$$\frac{N^\circ_{11}}{K_{11} + N^\circ_{11}} = \frac{N^\circ_{21}}{K_{21} + N^\circ_{21}}. \tag{3.6}$$

This equality is easy to check by substitution of Eqn. (3.3) into Eqn. (2.3).

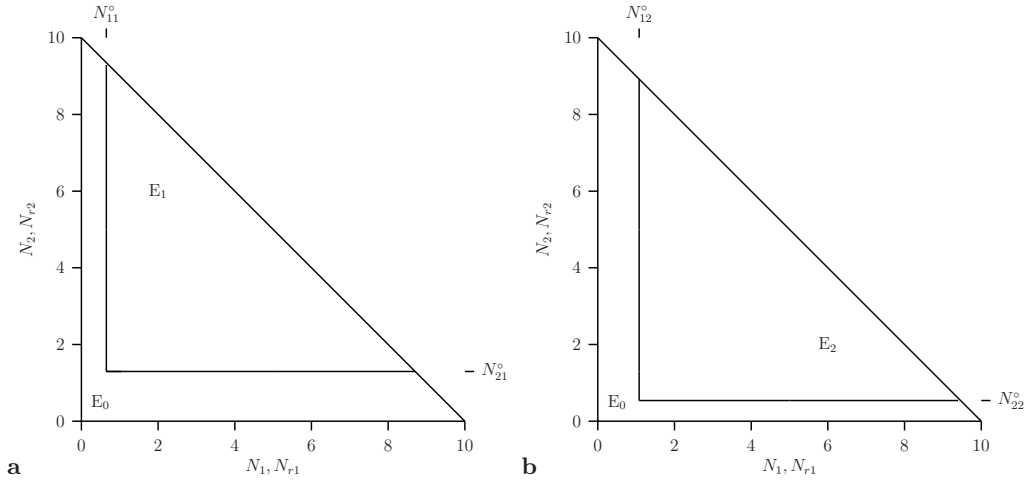

FIGURE 1. Resource quarter plane plots for the two one species—two resources PER-models: **a** for species $j = 1$ that is $N_2 = 0$, and **b** for species $j = 2$ that is $N_1 = 0$. For the sum of the two resources we take $N_{r1} + N_{r2} < 10$. The parameter values are given in Table 2. In region E_0 no species can persist and in regions E_j only species j exists. The curves are the zero net growth isocline ZNGI-curve.

3.1.2. Two species—two resources

For both species together, there are two zero-growth isoclines: one for each species. There are three different cases depending on the relative positions of these curves in the plane. When $N_{11}^\circ < N_{12}^\circ$ and $N_{21}^\circ < N_{22}^\circ$ species P_1 always wins; while when $N_{11}^\circ > N_{12}^\circ$ and $N_{21}^\circ > N_{22}^\circ$ species 2 always wins. In those cases the Tilman's-R* [29] rule holds saying: "The species that can survive at the lowest levels of a limiting resource will be the best competitor for that resource". For the parameter values given in Table 2 we have $N_{11}^\circ < N_{12}^\circ$ and $N_{21}^\circ > N_{22}^\circ$. Hence, the zero-growth isoclines of the two species intersect at the point N (see Fig. 2) where coexistence of both the species is possible. This equilibrium point is not on both of the two switching curves (straight lines through the origin) and therefore there is no co-limitation, that is both species are not limited by both resources simultaneously.

The resource quarter plane plot for the PER-model is shown in Fig. 2 for the two state variables N_1 and N_2 which are the densities of the ambient resources. In the resource quarter plane plots besides N_1 and N_2 also N_{r1} and N_{r2} are mentioned on the horizontal and vertical axis (see for instance [31]). This is since although the consumption vector is fixed by N_1 and N_2, the resource supply vector is also fixed by N_{r1} and N_{r2}. Both quantities, the ambient resource N_j and the inflow resource densities N_{rj} have the same dimension/unit and therefore there is one scale on each axis.

The parameter values are given in Table 2 where ϵ is a measure for the difference in the maximum growth and ingestion rate, respectively, for the two resources used by species 1. For species 2 the ingestion rates for both resources are entirely equivalent.

The position of the equilibrium point N, (N_1^*, N_2^*) is equal to the subsistence resource densities $(N_1^* = N_{12}^\circ, N_2^* = N_{21}^\circ)$ and therefore independent of the two parameters N_{r1} and N_{r2} forming the resource supply point. Denoting the species densities by P_1^* and P_2^* at the equilibrium point $(N_{12}^\circ, N_{21}^\circ)$, we have

$$(N_{r1} - N_{12}^\circ)D = I_{11} f_1^* P_1^* + I_{12} f_2^* P_2^* \,, \tag{3.7a}$$

$$(N_{r2} - N_{21}^\circ)D = I_{21} f_1^* P_1^* + I_{22} f_2^* P_2^* \,, \tag{3.7b}$$

$$Y(I_{11} + I_{21}) f_1^* = D + m_1 \,, \tag{3.7c}$$

$$Y(I_{12} + I_{22}) f_2^* = D + m_2 \,, \tag{3.7d}$$

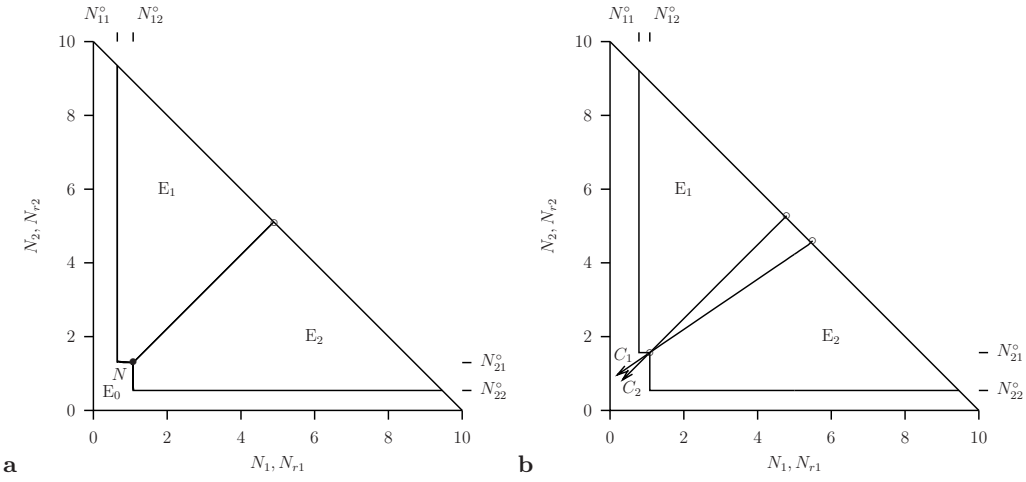

FIGURE 2. Resource quarter plane plots (N_1, N_2) for the PER-model: **a** for $\epsilon = 0$ and **b** for $\epsilon = 0.4$. On the hypotenuse the sum of the two resources is arbitrarily given by $N_{r1} + N_{r2} = 10$. In **a** the point N is coexistence equilibrium point. Hence there is no region where the two species can coexist. At the curve, the equilibrium is not unique. The parameter values are given in Table 2. Note that the slopes of the consumption vectors C_1 and C_2 are equal for $\epsilon = 0$.

where f_j^* means that the resource equilibrium values $(N_{12}^\circ, N_{21}^\circ)$ are substituted in the expressions for f_j in Eqs. (2.3), that is $f_j^* = f_j^{min}(N_{12}^\circ, N_{21}^\circ)$ and is given by:

$$f_1^* = \min\left(\frac{N_{12}^\circ}{K_{11} + N_{12}^\circ}, \frac{N_{21}^\circ}{K_{21} + N_{21}^\circ}\right) = \frac{D + m_1}{Y(I_{11} + I_{21})} , \tag{3.8a}$$

$$f_2^* = \min\left(\frac{N_{12}^\circ}{K_{12} + N_{12}^\circ}, \frac{N_{21}^\circ}{K_{22} + N_{21}^\circ}\right) = \frac{D + m_2}{Y(I_{12} + I_{22})} . \tag{3.8b}$$

These equations resemble those given by Eqs. (3.1). However, those equations were uncoupled, both species consume both resources without competition while here there is competition and both species consume simultaneously both resources N_1 and N_2. So far the calculation of the equilibrium point is done algebraically.

3.1.3. Graphical derivation

In this section we give a short graphical derivation of the results following Tilman [31] including the interpretation of consumption vectors and resource supply vectors. The consumption vector for each of the species j; $\mathbf{C}_j$ has two components, each representing the ingestion rate of one of the resources N_1 and N_2. These two consumption vectors are shown in Fig. 2**b** and defined as:

$$\mathbf{C}_j = \begin{pmatrix} I_{1j} \\ I_{2j} \end{pmatrix} f_j^* P_j^* . \tag{3.9}$$

Therefore I_{2j}/I_{1j} equals the slope of the consumption vector C_j. The resource supply vector $\mathbf{S}$ is given by the left hand side of Eqs. (3.7a) and (3.7b):

$$\mathbf{S}(N_{r1}, N_{r2}) = \begin{pmatrix} N_{r1} - N_1^* \\ N_{r2} - N_2^* \end{pmatrix} D . \tag{3.10}$$

So, at equilibrium the vectors balance and we have

$$\mathbf{S}(N_{r1}, N_{r2}) = \mathbf{C}_1 + \mathbf{C}_2 \ . \tag{3.11}$$

If one of the species, say 2 is extinct, the supply vector $\mathbf{S}$ balances the consumption vector $\mathbf{C}_1$ and vice verse. To each of these situations belongs a particular pair of resource supply points (N_{r1}, N_{r2}) indicated by an open circle in Fig. 2**b**.

With $\epsilon = 0$ (i.e. $I_{11} = I_{21}$ and $I_{12} = I_{22}$), both the consumption vectors (not shown in Fig. 2**a**) $\mathbf{C}_j$ for species $j = 1, 2$ coincide for the parameter values given in Table 2. This equilibrium occurs for the supply point indicated by the open circle at the hypotenuse in Fig. 2**a**. As a result, the two regions where either one or the other species (P_1 or P_2) wins, denoted by E_1 and E_2 are separated by a single line. This line originates from the equilibrium point N with resource densities N_1^* and N_2^*. The solutions for P_1^* and P_2^* are however, not unique. We return to the fact that this equilibrium point is degenerated in the next section.

The two consumption vectors Eqs. (3.9) which for $\epsilon = 0$ in Fig. 2**a** coincide at the equilibrium point N (not shown), do not coincide in general for $\epsilon \neq 0$. This is shown in Fig. 2**b** where $\epsilon = 0.4$. The consumption vectors for each of these species balance different resource supply vectors. The consumption vectors shown are those for the limiting cases for the mono-species solutions where $P_j^* = 0$ which forms a boundary of the regions indicated by E_j. The two related supply points are indicated with open circles on the hypotenuse. Within the wedge we have both E_1 and E_2

In Figs. 3**a-b** the resource quarter plane plots are shown for $\epsilon = 0.4$ and $\epsilon = -0.4$, respectively. The double vectors indicate the balance between the consumption vector and the supply vector. Assume that the supply point is on the hypotenuse. When the supply point is on the upper branch in the dark gray region, species 1 wins and the equilibrium is either on the vertical zero-growth isocline N_{11}° or on the horizontal growth curve N_{21}° terminating in the equilibrium point. Similarly, when the supply point is on the lower branch in the light gray region, species 2 wins and the equilibrium is either on the horizontal zero-growth isocline N_{22}° or on the vertical growth curve N_{12}° terminating in the equilibrium point.

When the supply point is in the intermediate interval in the dark gray region in panel 3**a** or in the white region in panel 3**b** there is coexistence at the equilibrium point. In panel 3**a** for $\epsilon = 0.4$ the equilibrium point is unstable and there is bistability, i.e. each of the species may win depending on the initial conditions. In panel 3**b** for $\epsilon = -0.4$ the equilibrium point is stable and there is co-existence. At this equilibrium point there is no co-limitation.

3.2. The bifurcation analysis

In this section we analyse the model (2.2) using techniques from nonlinear dynamical systems theory. This includes the derivation of expressions for the equilibrium points and the analysis of their stability. Thereafter, the dependency on parameters is studied whereby one or two parameters are varied. This yields critical parameter values were the asymptotic dynamical behavior changes qualitatively. These critical parameter values correspond to bifurcation points when one parameter is varied or curves of bifurcation points when two parameters are varied simultaneously in a two parameter bifurcation diagram. In the resource quarter plane plot along the axes the densities of ambient resources N_1 and N_2 are plotted (see for instance [30]) to fix the ambient resource point (N_1, N_2). However, to fix the resource supply point (N_{1r}, N_{2r}) the resource inflows densities N_{r1} and N_{r2} are taken along the same axes (see for instance [31]). In the two parameter bifurcation diagram only the resource inflow densities N_{r1} and N_{r2} are the bifurcation parameters and plotted along the axes.

The numerical bifurcation analysis results are calculated for Eqs. (2.2) with the parameter values given in Table 2. We used the numerical bifurcation package AUTO [5] to calculate and continue equilibria and their stability as well as bifurcation points (critical parameter values) or curves of bifurcation points when two parameters are varied simultaneously.

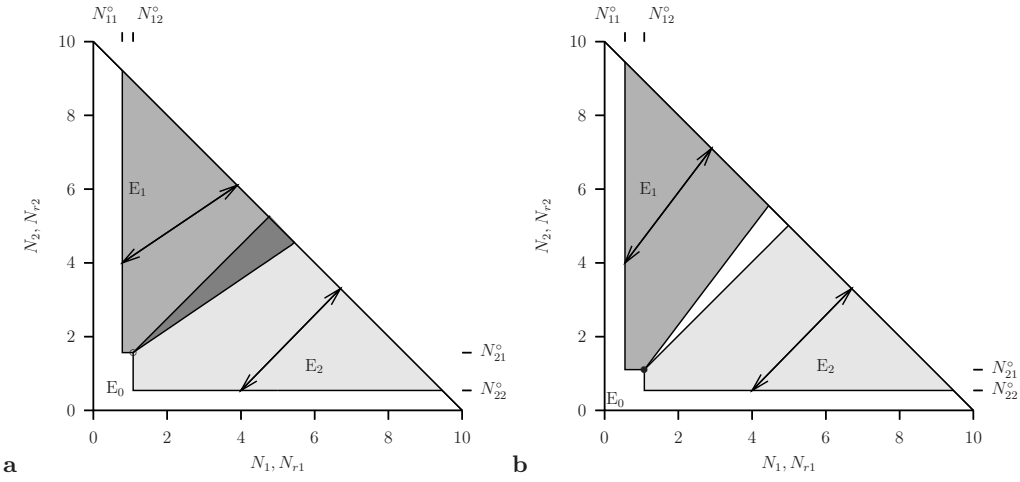

FIGURE 3. PER model: Resource quarter plane plot for the ambient resource densities N_1 and N_2 (see also Fig. 2). **a**: $\epsilon = 0.4$ and **b**: $\epsilon = -0.4$ and the other parameter values are given in Table 2. The coexistence equilibrium point is unstable (denoted by '$\circ$') for $\epsilon = 0.4$ and stable (denoted by '$\bullet$') for $\epsilon = -0.4$. The double vectors indicate the balance between the consumption vector and the supply vector. There is coexistence at the equilibrium point in the dark gray region in panel **a** (unstable and bistability) and in the white region in panel **b** (stable and co-existence).

3.2.1. Bifurcation analysis of the PER-model

The bifurcation diagram for the PER-model is shown in Fig. 4**b** for the two parameters N_{r1} and N_{r2} using the parameter values given in Table 2 with $\epsilon = 0$. For a direct comparison we again show the resource quarter plane plot in Fig. 4**a**. All special points and curves occur in both panels at the same place notwithstanding the fact that the quantities on the axes are different. In the following we will derive analytical expressions which indicate the existence of the equilibria E_1 and E_2. While these expressions are general, they can be numerically computed and plotted using specific parameter values for the model (2.2).

We study now the stability of the equilibrium solutions of Eqs. (3.7). The Jacobian matrix $\mathcal{J}$ of the two-resources–two species system (2.2) is given by:

$$\begin{pmatrix} -\frac{\partial(I_{11}f_1P_1+I_{12}f_2P_2)}{\partial N_1} - D & -\frac{\partial(I_{11}f_1P_1+I_{12}f_2P_2)}{\partial N_2} & -I_{11}f_1 & -I_{12}f_2 \\ -\frac{\partial(I_{21}f_1P_1+I_{22}f_2P_2)}{\partial N_1} & -\frac{\partial(I_{21}f_1P_1+I_{22}f_2P_2)}{\partial N_2} - D & -I_{21}f_1 & -I_{22}f_2 \\ Y(I_{11}+I_{21})\frac{\partial f_1}{\partial N_1}P_1 & Y(I_{11}+I_{21})\frac{\partial f_1}{\partial N_2}P_1 & Y(I_{11}+I_{21})f_1 - D - m_1 & 0 \\ Y(I_{12}+I_{22})\frac{\partial f_2}{\partial N_1}P_2 & Y(I_{12}+I_{22})\frac{\partial f_2}{\partial N_2}P_2 & 0 & Y(I_{12}+I_{22})f_2 - D - m_2 \end{pmatrix}. \tag{3.12}$$

3.2.1.1. Equilibrium $E_0 = (N_1^0, N_2^0, P_1^0, P_2^0) = (N_1^0, N_2^0, 0, 0)$: For the evaluation of the Jacobian matrix (3.12) at the trivial zero-equilibrium $E_0 = (N_1^\circ = N_{r1};\ N_2^\circ = N_{r2}$ and $P_1^\circ = P_2^\circ = 0)$ we obtain the following upper triangular matrix

$$\mathcal{J}|_{E_0} = \begin{pmatrix} -D & 0 & -I_{11}f_1^\circ & -I_{12}f_2^\circ \\ 0 & -D & -I_{21}f_1^\circ & -I_{22}f_2^\circ \\ 0 & 0 & Y(I_{11}+I_{21})f_1^\circ - D - m_1 & 0 \\ 0 & 0 & 0 & Y(I_{12}+I_{22})f_2^\circ - D - m_2 \end{pmatrix}_{E_0}, \tag{3.13}$$

where f° means that the equilibrium values are substituted in the expressions for f in Eqs. (2.3) or (2.4). The eigenvalues of this Jacobian matrix (3.13) determine the stability of the trivial equilibrium E_0. If all eigenvalues have a negative real part, E_0 is stable. Besides the two negative eigenvalues $-D$,

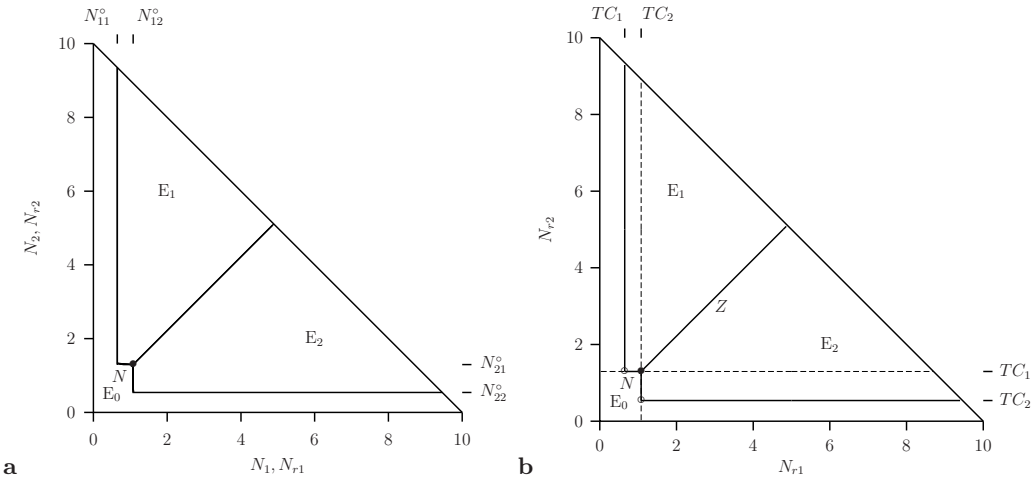

FIGURE 4. PER-model. **a**: Resource quarter plane plot for the ambient resource densities N_1 and N_2 (see also Fig. 2). **b**: the two-parameter bifurcation diagram with bifurcation parameters as the densities in the inflow N_{r1} and N_{r2}. The transcritical bifurcation curves TC_1, TC_2, and the double transcritical bifurcation curve Z (collision of TC_{12} and TC_{21}), are straight lines originating from a bifurcation point N which forms the organizing center. The parameter values are given in Table 2.

the two lower diagonal matrix elements are also eigenvalues whose signs determine the stability of the equilibrium E_0. A transcritical bifurcation related to a loss of stability of E_0 occurs, when one of those two eigenvalues changes its sign. Hence, the zero's of the following analytical expressions give the two transcritical bifurcation curves TC_j, respectively

$$Y(I_{1j} + I_{2j})f_j^\circ - D - m_j = 0\,. \tag{3.14}$$

In case of the Liebig formulation $f_j = f_j^{min}$ these equations are equal to those given in Eq. (3.1). We defined the subsistence resource densities N_{ij}° for $i = 1, 2$ and $j = 1, 2$ by Eq. (3.3).

Then we have for the transcritical bifurcations TC_j

$$\begin{cases} N_{r1} = N_{1j}^\circ\,, \forall N_{r2} \text{ if } & \frac{N_{1j}^\circ}{K_{1j}+N_{1j}^\circ} \le \frac{N_{2j}^\circ}{K_{2j}+N_{2j}^\circ} \\ N_{r2} = N_{2j}^\circ\,, \forall N_{r1} \text{ if } & \frac{N_{1j}^\circ}{K_{1j}+N_{1j}^\circ} > \frac{N_{2j}^\circ}{K_{2j}+N_{2j}^\circ} \end{cases}\,, \tag{3.15}$$

where $j = 1, 2$, so that these relationships define two horizontal and two vertical lines.

For low resource inflow both expressions on the left-hand sides in Eq. (3.14) will be negative and both populations go extinct and therefore we have a stable trivial zero solution E_0. For the PER-model (2.2) with (2.3), the bifurcation diagram where the two parameters (N_{r1}, N_{r2}) are the bifurcation parameters and $\epsilon = 0$ is shown in Fig. 4**b**. In this figure the relevant parts of these transcritical bifurcation curves TC_j where the trivial equilibrium E_0 looses its stability are shown as solid lines.

3.2.1.2. Equilibrium $E_1 = (\bar{N}_1, \bar{N}_2, \bar{P}_1, 0)$ and $E_2 = (\hat{N}_1, \hat{N}_2, 0, \hat{P}_2)$: If for $j = 1$ the expression on the left-hand side in Eq. (3.14) is zero and negative for $j = 2$ then we have a transcritical bifurcation point TC_1. Increasing the resource inflow N_{r1} (say $N_{r2} = 5$) in Fig. 4, the trivial zero equilibrium E_0 becomes unstable and the positive equilibrium E_1, with $\bar{P}_1 > 0$ and $\bar{P}_2 = 0$, becomes stable at the point $N_{r1} = N_{11}^\circ$. Increasing N_{r1} further unto a critical value, the expression on the left-hand side in Eq. (3.14) is zero at $N_{r1} = N_{12}^\circ$ for $j = 2$. This point is on the transcritical bifurcation curve TC_2 but because the other eigenvalue (the expression on the diagonal of the Jacobian matrix in Eq. (3.13) which

is also an eigenvalue,) is positive, the trivial zero equilibrium E_0 is unstable on both sides of this point. Consequently this critical point is irrelevant.

Starting from the point on the transcritical bifurcation TC_1 again and varying both N_{r1} and N_{r2} simultaneously gives the codimension-one transcritical bifurcation curve TC_1. This curve is a vertical line, described by Eq. (3.15) for $j = 1$. Lowering N_{r2} this line terminates at the switching bifurcation point $N_{r1} = N_{11}^{\circ}$ and $N_{r2} = N_{21}^{\circ}$ (indicated by a '°' in Fig. 4**b**) that is where co-limitation occurs. From this switching bifurcation point TC_1 continues at a right-angle until it terminates at the point N.

Similar, increasing the resource inflow N_{r2} at say $N_{r1} = 5$ crossing the transcritical bifurcation point TC_2 at $N_{r2} = N_{22}^{\circ}$ a stable positive equilibrium E_2, with $\hat{P}_2 > 0$ and $\hat{P}_1 = 0$ originates. Following the TC_2 curve which is a straight line that terminates at a second switching bifurcation point where $N_{r1} = N_{12}^{\circ}$ and $N_{r2} = N_{22}^{\circ}$. The TC_2 continues at a right angle and terminates at point N. At this codimension-two point N the transcritical bifurcations TC_1 and TC_2 intersect, and both equations in Eqs. (3.14) for $j = 1, 2$, are satisfied simultaneously, when

$$N_{r1} = N_{12}^{\circ} \quad \text{and} \quad N_{r2} = N_{21}^{\circ} \; . \tag{3.16}$$

Now suppose that one species invaded the resource system, e.g. $\bar{P}_1 > 0$ and $\bar{P}_2 = 0$. At that equilibrium E_1 we have

$$0 = (N_{r1} - \bar{N}_1)D - I_{11}\bar{f}_1\bar{P}_1 \; , \tag{3.17a}$$
$$0 = (N_{r2} - \bar{N}_2)D - I_{21}\bar{f}_1\bar{P}_1 \; , \tag{3.17b}$$
$$0 = \big(Y(I_{11} + I_{21})\bar{f}_1 - D - m_1\big)\bar{P}_1 \; . \tag{3.17c}$$

The Jacobian matrix evaluated at equilibrium E_1 reads, using $\bar{P}_2 = 0$,

$$\mathcal{J}|_{E_1} = \begin{pmatrix} -I_{11}\frac{\partial f_1}{\partial N_1}P_1 - D & -I_{11}\frac{\partial f_1}{\partial N_2}P_1 & -I_{11}f_1 & -I_{12}f_2 \\ -I_{21}\frac{\partial f_1}{\partial N_1}P_1 & -I_{21}\frac{\partial f_1}{\partial N_2}P_1 - D & -I_{21}f_1 & -I_{22}f_2 \\ Y(I_{11}+I_{21})\frac{\partial f_1}{\partial N_1}P_1 & Y(I_{11}+I_{21})\frac{\partial f_1}{\partial N_2}P_1 & 0 & 0 \\ 0 & 0 & 0 & Y(I_{12}+I_{22})f_2 - D - m_2 \end{pmatrix}_{E_1} \; . \tag{3.18}$$

We can now analyse the two transcritical bifurcation curves TC_{21} (TC_{12}) where a competitor species 2 (1) starts to invade the system with the two resources and the species 1 (2). These two transcritical bifurcations TC_{12} and TC_{21} correspond mathematically to the loss of stability of the afore mentioned equilibria E_1 and E_2, respectively, at a critical point where one eigenvalue is zero.

At the transcritical bifurcation points TC_{21} the equilibrium E_1, i.e. $\bar{P}_1 > 0, \bar{P}_2 = 0$ looses its stability. The set of Eqs. (3.17) determine the two unknown equilibrium values $\bar{N}_1$ and $\bar{N}_2$. The following conditions determine the transcritical bifurcation point TC_{21}

$$0 = (N_{r1} - \bar{N}_1)D - I_{11}\bar{f}_1\bar{P}_1 \; , \tag{3.19a}$$
$$N_{r2} = \bar{N}_2 + \frac{I_{21}}{I_{11}}(N_{r1} - \bar{N}_1) \; , \tag{3.19b}$$
$$0 = Y(I_{11} + I_{21})\bar{f}_1 - D - m_1 \; , \tag{3.19c}$$
$$0 = Y(I_{12} + I_{22})\bar{f}_2 - D - m_2 \; , \tag{3.19d}$$

The latter two equations are independent of N_{r1} and N_{r2} and consequently also the two equilibrium values $\bar{N}_1$ and $\bar{N}_2$. The explicit expression for N_{r2} as a function of N_{r1} in Eq. (3.19b) shows that the transcritical bifurcation curve TC_{21} in the (N_{r1}, N_{r2}) diagram is a straight line with slope I_{21}/I_{11}. This slope is equal to the slope of the consumption vector $\mathbf{C}_1$ (see Eq. (3.9)).

In the same way we can describe the transcritical bifurcation curve TC_{12} of equilibrium E_2, i.e. $\hat{P}_1 = 0, \hat{P}_2 > 0$, by the following conditions:

$$0 = (N_{r1} - \hat{N}_1)D - I_{12}\hat{f}_2\hat{P}_2 \ , \tag{3.20a}$$

$$N_{r2} = \hat{N}_2 + \frac{I_{22}}{I_{12}}(N_{r1} - \hat{N}_1) \ , \tag{3.20b}$$

$$0 = Y(I_{11} + I_{21})\hat{f}_1 - D - m_1 \ , \tag{3.20c}$$

$$0 = Y(I_{12} + I_{22})\hat{f}_2 - D - m_2 \ . \tag{3.20d}$$

From Eq. (3.20b) we find that, TC_{12} is a straight line N_{r2} as a function of N_{r1} with slope I_{22}/I_{12} and this is equal to the slope of the consumption vector $\mathbf{C}_2$.

3.2.1.3. Equilibrium $E_{12} = (N_1^*, N_2^*, P_1^*, P_2^*)$: Equilibrium equations for the equilibrium E_{12} with two coexisting species with densities $P_1^* > 0$, $P_2^* > 0$. Eqs. (3.7) yield:

$$\begin{pmatrix}(N_{r1} - N_1^*)D\\(N_{r2} - N_2^*)D\end{pmatrix} = \begin{pmatrix}I_{11}\ I_{12}\\I_{21}\ I_{22}\end{pmatrix}\ \begin{pmatrix}f_1^*P_1^*\\f_2^*P_2^*\end{pmatrix} \ , \tag{3.21}$$

or

$$\begin{pmatrix}f_1^*P_1^*\\f_2^*P_2^*\end{pmatrix} = \begin{pmatrix}I_{11}\ I_{12}\\I_{21}\ I_{22}\end{pmatrix}^{-1}\ \begin{pmatrix}(N_{r1} - N_1^*)D\\(N_{r2} - N_2^*)D\end{pmatrix} \ , \tag{3.22}$$

where N_i^*, $i = 1, 2$ directly follow from Eqs. (3.8). For the 2-dimensional non-homogeneous linear system, where $f_1^*P_1^*$ and $f_2^*P_2^*$ are the two unknowns and all coefficients related to N_1^* and N_2^* are known, Linear Algebra says that

1. if the corresponding homogeneous system has only the zero solution, then there is a unique solution for all values of the left-hand side of (3.21). Then the matrix with the ingestion rates I_{ij} is nonsingular and this occurs for instance when $\epsilon \neq 0$ in Table 2.
2. if the corresponding homogeneous system has a non-zero solution, then
   (a) there are values for the left-hand side for which system (3.21) does not have a solution: This does not occur here because the mass-balance system is bounded.
   (b) whenever a solution of system (3.21), exists, it is not unique, since only the sum of P_1^* and P_2^* is fixed, but not the two state variables separately. In this case the matrix with the ingestion rates I_{ij} is singular and this occurs for instance when $\epsilon = 0$ in Table 2.

For the reference parameter set given in Table 2 with $\epsilon = 0$, that is $I_{11} = I_{21} = 1.25$ and $I_{12} = I_{22} = 1.05$, both expressions (3.19b) and (3.20b) are satisfied simultaneously. In this case the two transcritical bifurcations TC_{12} and TC_{21} coincide and form a double transcritical bifurcation line Z. Eqs. (3.8**a**) and (3.8**b**) determine $f_1^* \neq f_2^*$ and the equilibrium values N_1^* and N_2^* are the unique solution of two linear equations. However, the matrix in Eq. (3.21) is singular and is not invertible. Hence, in this degenerate case the corresponding homogeneous system has one non-zero solution for P_1^* and P_2^*. This means that there is coexistence of P_1 and P_2 and indeed this equilibrium is not unique. For other parameter value combinations in the right upper part of the bifurcation diagram not on the Z line, illustrated in Fig. 4 there is no coexistence.

For $\epsilon = \pm 0.4$ the two-parameter bifurcation diagrams are shown in Fig. 5. The two transcritical bifurcations TC_{12} and TC_{21} differ now and do not coincide like in Fig. 4. Note that transcritical bifurcation curve TC_{12} has for both cases the same slope, $I_{22}/I_{12} = 1$ and is perpendicular to the hypotenuse. The transcritical bifurcation curve TC_{21} lies on the two opposite sides of TC_{12} for $\epsilon = \pm 0.4$ respectively. There is bistability for $\epsilon = +0.4$ (see Fig. 5**a**) and coexistence for $\epsilon = -0.4$ (see Fig. 5**b**). With respect to the bifurcation pattern the only difference between the two cases $\epsilon = \pm 0.4$ is the relative position of the two transcritical bifurcation curves TC_{21} and TC_{12}. For $\epsilon = 0.4$ the intersection point of TC_{12} with the hypotenuse occurs for a lower N_{r1} value than that for TC_{21}. For $\epsilon = -0.4$ it is just the reverse. The curve

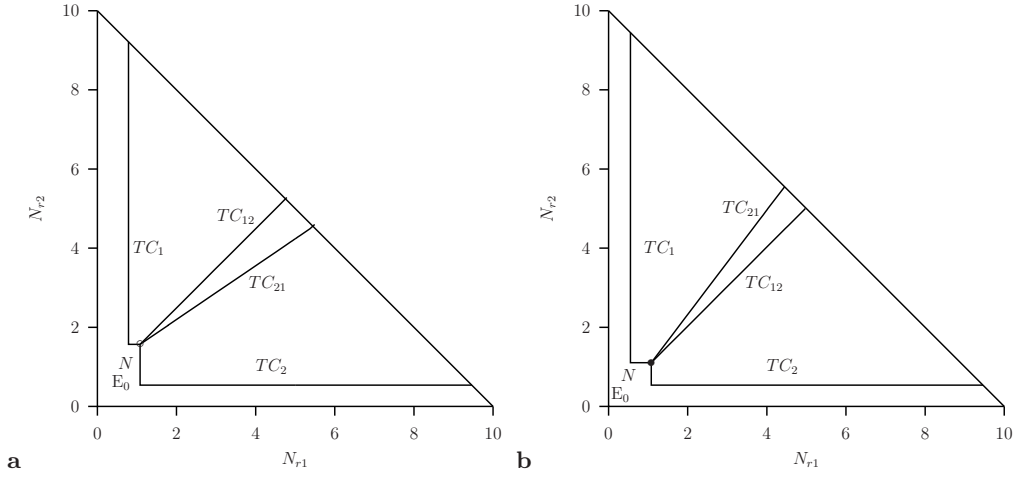

FIGURE 5. PER model. Two-parameter bifurcation diagram (N_{r1}, N_{r2}), with the Liebig's competitive interaction between the two species. **a**: $\epsilon = 0.4$ and **b**: $\epsilon = -0.4$ in Table 2. Point N is the coexistence equilibrium point unstable for $\epsilon = 0.4$ and stable for $\epsilon = -0.4$. There two transcritical bifurcation curves are TC_{12} and TC_{21}. When the inflow of the two resources is in between these two lines there is bistability in panel **a** with $\epsilon = 0.4$ and stable coexistence in panel **b** with $\epsilon = -0.4$.

TC_{21} is described by Eq. (3.19b) and TC_{12} by Eq. (3.20b). Since both curves intersect at the organizing center N the position on the hypotenuse is uniquely determined by the two slopes, that is I_{21}/I_{11} versus I_{22}/I_{12} and we have bistability when $I_{22}/I_{12} < I_{21}/I_{11}$ and stable coexistence when $I_{22}/I_{12} > I_{21}/I_{11}$. For the parameter values in Table 2 we have $I_{22}/I_{12} = 1$ and $I_{21}/I_{11} = 1 + \epsilon/1.25$. So, for $\epsilon > 0$ we have $I_{22}/I_{12} < I_{21}/I_{11}$, i.e. bistability (see Fig. 5**a**) and for $\epsilon < 0$ we have $I_{22}/I_{12} > I_{21}/I_{11}$ which implies stable coexistence (see Fig. 5**b**).

To illustrate the different transcritical bifurcations, we now show one-parameter bifurcation diagrams where the resource inflow density is varied. There are two different resource inflow densities N_{ri}, $i = 1, 2$ and in order to get a one-parameter diagram we vary both simultaneously such that $N_{r1} + N_{r2} = 10$, that is along the hypotenuse of the two-parameter bifurcation diagrams Figs. 4 and 5. This links the two-parameter and the one-parameter bifurcation diagrams, since now the densities of the resources and species are shown completing the available information about the state of the system depending on the resource supply ratio.

In Fig. 6**a** the one-parameter bifurcation diagram for $\epsilon = 0$ is shown. For comparison the accompanying two-parameter diagram is shown in Fig. 6**b** (same as Fig. 4**b**). Since both resources are essential, both species are extinct for $N_{r1} = 0$ and $N_{r1} = 10$ because then $N_{r2} = 0$. By increasing N_{r1} we move along the hypotenuse in the two-parameter diagrams and pass the various transcritical bifurcations: TC_1, TC_2, Z, TC_{12}, TC_{21}. Below TC_1 we have the stable equilibrium E_0, between TC_1 and Z, equilibrium E_1 is stable and between Z and TC_2 equilibrium E_2 is stable and finally above TC_2 equilibrium E_0 becomes stable again. Note that some bifurcations plotted are not relevant for $N_{r1} + N_{r2} = 10$ but become relevant when the sum is smaller, for instance $N_{r1} + N_{r2} < N_{12}^{\circ} + N_{21}^{\circ}$ when point N lies above the hypotenuse. We emphasize again that along the line Z the equilibrium values of the populations are not unique.

Fig. 6**b** depicts that in regions '1' and '3' the resource N_1 is limiting for equilibrium E_1 and E_2 respectively, and in regions '2' and '4' the resource N_2 for equilibrium E_1 and E_2 respectively. These regions are separated by line Z and the two lines indicated by double arrows where both resources are co-limiting. Note that these curves are not "real" bifurcation curves. At these curves the elements of the Jacobian matrix are discontinuous with respect to the bifurcation parameters N_{r1} and N_{r2}. This is due

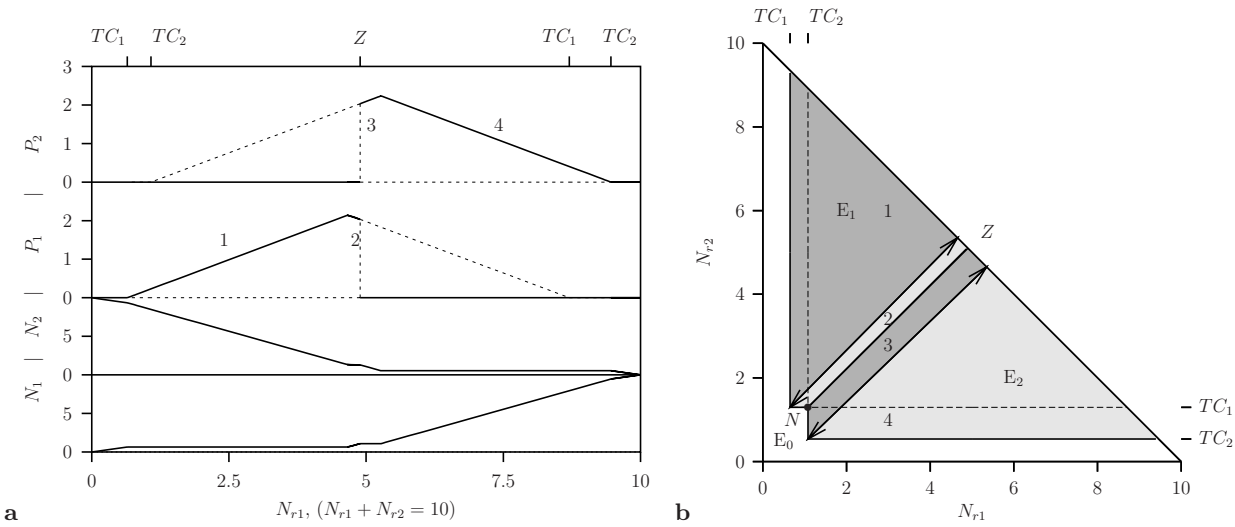

FIGURE 6. PER model. **a**: One-parameter bifurcation diagrams with equilibrium values of the resource densities N_1, N_2, and the species densities P_1, P_2. The bifurcation parameter is the density in the inflow N_{r1} such that $N_{r1} + N_{r2} = 10$. **b** the two-parameter bifurcation diagram with bifurcation parameters N_{r1} and N_{r2}. The transcritical bifurcation curves are TC_1, TC_2, and the double transcritical bifurcation curve is Z (collision of TC_{12} and TC_{21}). The two double arrows indicate the balance between the consumption vector and the supply vector where there is co-limitation. In regions '1' and '3' resource N_1 is limiting for equilibrium E_1 and E_2 respectively, and in regions '2' and '4' resource N_2 for E_1 and E_2 respectively.

to the minimum operator in the Liebig's minimum law, in Eq. (2.3). The curves form switching points where the other resource becomes limiting. At these switching points the equilibrium values for both species: P_1^* and P_2^* are at a maximum in Fig. 6**b**, where the species solution curves are continuous but the derivative with respect to the bifurcation parameter is discontinuous.

The one-parameter bifurcation diagrams for $\epsilon = \pm 0.4$ are shown in Fig. 7. The corresponding two parameter diagrams are shown in Fig. 5. The main difference with the degenerate case $\epsilon = 0$ is that there is an interior equilibrium in a finite interval around $N_{r1} = 5$. In Fig. 7**a** with $\epsilon = 0.4$ this equilibrium is unstable and we have bistability between the two transcritical bifurcation TC_{12} and TC_{21}. These two transcritical bifurcations mark the endpoints of a hysteresis loop when N_{r1} and N_{r2} are varied. Observe that when N_{r1} is decreased crossing TC_{12} species 2 suddenly goes extinct without any warning. Species 1 can invade below TC_{12} and out-competes species 2. In Fig. 7**b** with $\epsilon = -0.4$ the interior equilibrium is stable and we obtain coexistence between TC_{21} and TC_{12}.

Comparing Fig. 5**a** with Fig. 5**b** shows that the transcritical bifurcations TC_{12} and TC_{21} for $\epsilon = \pm 0.4$ differ. Those in Fig. 5**a** are sometimes called catastrophic for the following reason: Close to the bifurcation point where the two resources–one species system (e.g. N_1, N_2, P_1) is stable, a small perturbation of N_{r1} (and also N_{r2}) leads to convergence to the resources–competitor system (e.g. N_1, N_2, P_2) where the density of the competitor P_2 becomes substantially large. By contrast those bifurcations in Fig. 5**b** are called non-catastrophic. Now a perturbation of N_{r1} (and also N_{r2}) leads to convergence to a stable system where the invading species appears with a small density and coexists with the other species. Hence, when a catastrophic bifurcation is passed, the long-term dynamics changes abruptly, i.e. another species becomes suddenly dominant, while passing a non-catastrophic bifurcations leads only to slight changes in the population densities.

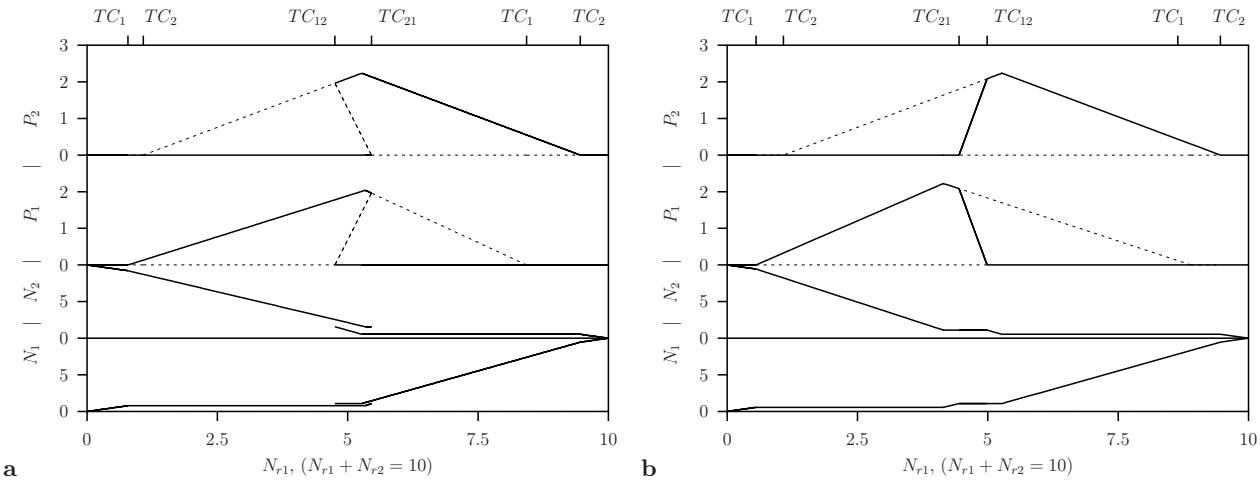

FIGURE 7. One-parameter bifurcation diagrams for the PER-model with equilibrium values of the resource densities N_1, N_2, and the species densities P_1, P_2. **a**: $\epsilon = 0.4$ and **b**: $\epsilon = -0.4$ in Table 2. The bifurcation parameter is the density in the inflow N_{r1} such that $N_{r1} + N_{r2} = 10$. Perturbations of Fig 6 with bistability (**a**) and coexistence (**b**) in small (N_{r1}, N_{r2})-interval between the two transcritical bifurcations TC_{12} and TC_{21}.

For resource densities in the inflow N_{r1} and N_{r2} between the two transcritical bifurcation TC_{12} and TC_{21} the matrix with the ingestion rates I_{ij} (see Eq. (3.21)) is nonsingular, i.e. $\epsilon \neq 0$. Therefore there exists a unique equilibrium E_{12} with the following stability properties:

1. Equilibrium E_{12} is stable when the two equilibria E_1 and E_2 are unstable,
2. Equilibrium E_{12} is unstable when the two equilibria E_1 and E_2 are stable.

3.3. Comparison of the two approaches

Here we compare the resource quarter plane analysis approach with the bifurcation analysis approach. The resource quarter plane plot in Fig. 4**a** shows zero-growth isoclines of both species in the ambient resource space. At each point on the zero-growth isoclines where one species persists, the *resource supply vector* balances the *consumption vector*. The intersection of the zero-growth isoclines, gives the ambient resource densities at which equilibrium coexistence of both the species is possible. This method shows the possibility of various outcomes of competition: stable coexistence of the two species, one of the species wins depending on the initial condition (bistability) and always one of the two species wins (competitive exclusion) (see also Fig. 2**b**).

The resource quarter plane plot in Fig. 4**a** is spanned by two state variables, namely the ambient resource densities N_1 and N_2. In this plane Eq. (3.11) is a necessary condition to have an equilibrium so that the right-hand sides of Eqs. (2.2a) and (2.2b) are zero independently of N_{r1} and N_{r2}. In general this is not sufficient because also the right-hand sides of Eqs. (2.2c) and (2.2d) have to be zero. However, in the PER model Eq. (3.11) is also sufficient because when the right-hand sides of Eqs. (2.2c) and (2.2d) are zero this fixes N_1^* and N_2^* and the resulting expressions are independent of N_{r1} and N_{r2} (see Eqs. (3.8)).

The two-parameter plots obtained by a bifurcation analysis Fig. 4**b** are spanned by two parameters describing the inflow densities N_{r1} and N_{r2} of the resources. In the latter diagram the curves indicating the invasion of one species into the empty system correspond to curves of transcritical bifurcations of the trivial equilibrium $E^0 = (N_1^0, N_2^0, P_1^0, P_2^0) = (N_1^0, N_2^0, 0, 0)$. Crossing these transcritical bifurcations TC_1 or TC_2 by varying the resource inflow densities N_{r1} and/or N_{r2} leads to the new stable equilibrium $E_1 = (\bar{N}_1, \bar{N}_2, \bar{P}_1, 0)$ or $E_2 = (\hat{N}_1, \hat{N}_2, 0, \hat{P}_2)$ where either P_1 or P_2 persists respectively.

Comparing the bifurcation diagram in Fig. 4**b** with Fig. 6**b** shows that only parts of the transcritical bifurcations are relevant. That occurs when at the critical point one eigenvalue is zero but there are one or multiple positive eigenvalues that do not change sign at the bifurcation point. This is especially true for TC_1 and TC_2.

In a bifurcation analysis approach the stability of an equilibrium is studied by linearisation in the equilibrium point whereby the sign of the dominant eigenvalue of the Jacobian matrix is decisive. However, due to the minimum operator in the Liebig's minimum law, in Eq. (2.3) the elements of the Jacobian matrix are discontinuous with respect to the bifurcation parameters N_{r1} and N_{r2} at the switching point, that is when the other resource becomes limiting. As a consequence also the eigenvalues are discontinuous, but the governing equations and the equilibrium values are continuous. In Fig. 6**b** switching bifurcation points (denoted by a '$\circ$') occur at the two right-angle points where co-limitation occurs. The discontinuities in the Jacobian matrix elements explain why at the two switching bifurcation points the relevant transcritical bifurcation curve, the solid curve in Fig. 6**b**, is non-smooth. Hence the two switching points at the right-angle point, act as codimension-two points similar to the point N being the terminal point of the double transcritical bifurcation curve Z.

Two more bifurcations are important for the dynamics of the system, which are related to the emergence of the interior equilibrium $\mathrm{E}_{12} = (N_1^*, N_2^*, P_1^*, P_2^*)$ which is either stable (coexistence) or unstable (competitive exclusion). From Eq. (3.19b) the expression for TC_{21}, we derive that

$$\bar{N}_2 = N_{r2} + \frac{I_{21}}{I_{11}}(\bar{N}_1 - N_{r1}) \; . \tag{3.23}$$

Similarly we have for TC_{12},

$$\hat{N}_2 = N_{r2} + \frac{I_{22}}{I_{12}}(\hat{N}_1 - N_{r1}) \; . \tag{3.24}$$

Furthermore, at point N we have $N_i^* = N_{ri}$ and $P_j^* = 0$ for $i = 1, 2$ and $j = 1, 2$. Using the expressions (3.9) with $j = 1$ or $j = 2$ and (3.10,3.11) this explains why in Fig. 2**b** and Fig. 5**a** the wedge in which either stable coexistence or bistability can be observed, is the same since the two curves start in the common point N and the slopes of the curves are pairwise for $j = 1, 2$ the same, namely I_{21}/I_{11} and I_{22}/I_{12}, respectively.

Which of the two different behaviors is obtained depends on the relative position of the two transcritical bifurcation curves or equivalently the slopes of the curves which correspond to the consumption vectors. The one-parameter bifurcation diagrams in Figs. 6**a** deliver directly information not only about the densities of the resources N_i but also of the species j and also whether coexistence or bistability occurs.

In the resource quarter plane plot Fig. 4**a** the point where coexistence of the two species E_{12} is possible, is labeled by N. This is at the same time the intersection point of the zero-growth isoclines. In the bifurcation diagram Fig. 4**b** the point N marks the intersection point of all transcritical bifurcations. Hence, this point is of particular importance as it is the organizing center of the dynamics.

3.4. Numerical bifurcation analysis of the COM-model

The bifurcation analysis approach can also be applied when the resources are interactively-essential or complementary instead of perfect-essential. To illustrate this we analyse in this section the COM-model Eq. (2.2) with the trophic interactions described by the complementary resource formulation Eq. (2.4). Part of the analytical results derived in the previous section hold also for this model. An important difference is that in the PER-model for each species co-limitation does occur in specific situations. However, the growth of both the species are never co-limited, while in the COM-model both the species are always co-limited.

Below we only give the numerical analysis results. The parameter values are given again in Table 2. The one parameter bifurcation diagram is shown in Fig. 8**a** and the two parameter diagram in Fig. 8**b**. Let us compare the two-parameter bifurcation diagram in Fig. 6**b** and Fig. 8**b** and the one parameter

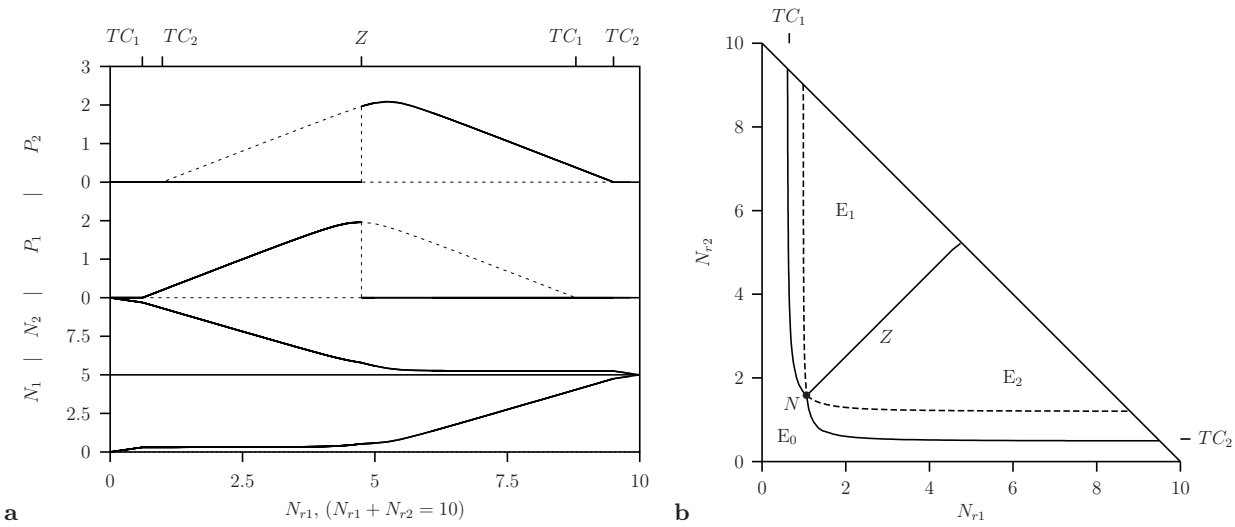

FIGURE 8. COM model. **a**: One-parameter bifurcation diagrams with equilibrium values of the resource densities N_1, N_2, and the species densities P_1, P_2. The bifurcation parameter is the density in the inflow N_{r1} such that $N_{r1} + N_{r2} = 10$. **b** the two-parameter bifurcation diagram with bifurcation parameters the densities in the inflow N_{r1} and N_{r2}. The transcritical bifurcation curves are TC_1, TC_2, and the double transcritical bifurcation curve is Z (collision of TC_{12} and TC_{21}).

bifurcation diagram in Fig. 6**a** and Fig. 8**a** for the two different modeling approaches. Both points N in Fig. 6**b** and Fig. 8**b**, i.e. the intersection of all possible bifurcation curves, serve as the organizing center of all different dynamical regimes. Firstly, we observe that the sharp changes in the perfect essential resource formulation (right-angle corners) are smoothed when the resources are considered to be complementary (round corner). Secondly, we note that for complementary resources co-limitation is always present.

In general the analysis of both models gives rise to a similar dynamics. For $\epsilon = 0$ we find the same degenerate behavior, represented by the coincidence of the two transcritical bifurcation lines TC_{21} and TC_{12} leading to a double transcritical bifurcation Z in which the population densities P_1 and P_2 are not unique. The results for the two model versions PER and COM, in the non-degenerated cases where $\epsilon \neq 0$ are similar in the same way as for $\epsilon = 0$ and are not shown here. Again the two cases $\epsilon = \pm 0.4$ give regions for the resource supply ratio where either stable coexistence or bistability occurs.

The one-parameter bifurcation diagrams for the two models, where N_{r1} is varied such that $N_{r1}+N_{r2} = 10$, are shown in Fig. 6**a** and Fig. 8**a**. The sharp changes in the perfect-essential resources formulation, due to the minimum operator, are smoothed in the interactively-essential resources formulation. Therefore the Jacobian matrix is always continuous and the transcritical bifurcation curves TC_1 and TC_2 are smooth curves which intersect at point N.

4. Discussion

In this paper we developed a framework for analysing resource competition models based on bifurcation theory. To elaborate the methodology we readdressed the problem of competition of two species for two resources in a chemostat. In the perfect-essential resources case (the PER-model) where one resource is limiting, the problem has been tackled already in the literature for various competition models [8, 13, 29, 30]. To illustrate that our approach can also be used for other model formulations we analysed the competition model with interactively-essential resources (the COM-model) in which co-limitation is always present.

The most prominent approach to analyse the model with perfect-essential resources is the graphical method by Tilman [29, 30] which is represented in resource quarter plane plots. We have demonstrated that the results obtained by Tilman can be analytically derived in terms of bifurcation theory. Based on a rigorous mathematical analysis we show that we obtain similar plots as the well-known resource quarter plane plots. This analysis reveals the conditions under which the resource quarter plane plots approach works, namely that the dynamics in the two-dimensional state space spanned by the ambient resource densities is sufficient to draw conclusions about the dynamics in the four-dimensional state space.

It is important to stress that the Monod/Liebig model [29, 30] formulation Eq. (2.1), possesses a peculiarity due to the Liebig's minimum law. In the classical formulation only the growth dynamics of the limiting resource is taken into account and not that of the non-limiting resource. For this reason we adapted the Monod/Liebig model to take the mass balance into account. In our mass balance model formulation (2.2) the resource dynamics contains both the consumption of the limiting and the non-limiting resources. Our results show that this adaption does not change the qualitative dynamics, but the quantitative values for the population densities in equilibrium are different. The advantage of the mass-balance formulation (2.2) is that we can also use it when both resources are always co-limiting as in the COM-model.

In the PER-model the elements in the Jacobian matrix and therefore also the eigenvalues are discontinuous with respect to the bifurcation parameters N_{r1} and N_{r2} at switching points. Consequently at these switching points the stability of the equilibrium point changes abruptly. Therefore at the right-angle corners in Fig. 6**b** where co-limitation occurs, the relevant transcritical bifurcation curve is also non-smooth due to an exchange of the transcritical bifurcation curves TC_1 and TC_2. Since this phenomenon does not occur in the COM-model because the functional response (2.4) is smooth, also the transcritical bifurcation curves in Fig. 6**b** are smooth are the curves where the switching takes place and regions with different limiting resources given in Fig. 6**b** are missing. Note that in both models at the codimension-two point N being the terminal point of the Z-curve, the relevant parts of transcritical bifurcation formed by TC_1 and TC_2 join at point N at a right-angle.

There is an increasing evidence that co-limitation is an important factor for the growth of many species [26]: hence it is important to extend the analysis of the outcome of competition to other functional responses taking co-limitation into account. Therefore we analyse besides the widely studied PER-model where at each time one resource is limiting, the COM-model, where two resources are co-limiting (see also [11]). The analysis of the two different kinds of models illustrates all the similarities between the graphical approach by Tilman and the rigorous bifurcation analysis. On the other hand we demonstrate in this way that the bifurcation analysis approach is more general since it can be applied to more complicated community models where possibly also non-equilibrium dynamic behaviour occurs.

In [26] these two model formulations are compared by experimental testing. In the experimental set-up a freshwater herbivore (*Daphnia magna*) feeds on two potentially limiting nutrients (cholesterol and eicosapentaenoic acid). For the growth rate of the herbivore they use for perfect essential resources Eq. (2.3) from [29,30] (the PER-model) and for interactively-essential resources Eq. (2.4) from [18,24] (the COM-model). Based on their experiment and results in [26] the authors hypothesize that co-limitation is a common phenomenon in nature not only for plants, but also for herbivorous consumers, as they are particularly sensitive to constraints in food quality. In [33] Tilman showed that for plants with foraging plasticity should lead to interactively-essential resources based on optimal foraging theory. This shows the relevance of the new results we obtained for the COM-model.

While the resource quarter plane plot approach depends crucially on special features of the model, the bifurcation analysis does not and it can be applied for a much larger class of models. For simple models analytical techniques suffice but for complex models one has to rely on numerical bifurcation analysis using computer packages such as AUTO [5] and MatCont [4]. To illustrate the model behaviour we varied the resource supply ratio as a bifurcation parameter in one-parameter bifurcation diagrams whereby all four state variables are plotted. The quantities along the axes in the two-parameter bifurcation diagrams are model parameters and no state variable is plotted. In other two-parameter bifurcation diagrams the

resource supply ratio together with the dilution rate or one of the other physiological parameters could be varied.

The bifurcation analysis approach can in general, be applied to a large class of competition models involving different functional responses as well as multiple resources and multi-species. Additionally, the analysis can be extended to models which not only exhibit equilibria but also oscillatory dynamics either by intrinsic instabilities shown by an ecosystem or by diurnal or seasonal forcing. Though the analysis and the numerical analysis become much more complicated.

Competition is also a crucial aspect of the assembly of ecological communities [22] and of the adaptive dynamics approach in evolution [7, 23]. In each step of the community assembly process a new species competes with the community species. When successful it either replaces one or more species, that are then removed from the community or extends the community. In adaptive dynamics mutant populations compete with the resident population on the evolutionary time scale. The outcome of the competition for resources between the mutant population and the resident population determines whether the population adapts. Our approach can also be used to study these issues in the assembly of ecological communities [15] and in adaptive dynamics in evolution [28].

Acknowledgements. We would like to thank Bas Kooijman for valuable discussions. One of the authors (P.S.D) thanks the *Alexander von Humboldt Foundation* for financial support in form of a postdoctoral fellowship.

References

[1] A. Ajbar, K. Alhumaizi. *Dynamics of the Chemostat: A Bifurcation Theory Approach.* Boca Raton FL, Taylor & Francis Group, CRC Press, 2012.

[2] B.C. Baltzis, A.G. Fredrickson. *Limitation of growth rate by two complementary nutrients: Some elementary but neglected considerations.* Biotechnol. Bioeng., 31 (1988), 75–86.

[3] A. Cunningham, R.M. Nisbet. *Transients and oscillations in continuous culture.* In M.J. Bazin (ed), Mathematics in Microbiology, pages 77–103, London, Academic Press, 1983.

[4] A. Dhooge, W. Govaerts, Yu.A. Kuznetsov. *Matcont: A MATLAB package for numerical bifurcation analysis of ODEs.* ACM T. Math. Software, 29 (2003), 141–164.

[5] E.J. Doedel, B. Oldeman. *Auto 07p: Continuation and bifurcation software for ordinary differential equations.* Technical report, Concordia University, Montreal, Canada, 2009.

[6] G.F. Gause. *The Struggle for Existence.* Hafner Publishing, New York, 1969.

[7] S.A.H. Geritz, É. Kisdi, G. Meszéna, J.A.J. Metz. *Evolutionarily singular strategies and the adaptive growth and branching of the evolutionary tree.* Evol. Ecol., 12 (1998), 35–57.

[8] J.P. Grover. *Resource Competition.* Population and Community Biology series. Chapman & Hall, London, 1997.

[9] J. Guckenheimer, P. Holmes. *Nonlinear Oscillations, Dynamical Systems and Bifurcations of Vector Fields.* volume 42 of Applied Mathematical Sciences. Springer-Verlag, New York, 2 edition, 1985.

[10] G. Hardin. *The competitive exclusion principle.* Science, 131:3409 (1960), 1292–1297.

[11] W.S. Harpole, J.T. Ngai, E.E. Cleland, E.W. Seabloom, E.T. Borer, M.E.S. Bracken, J.J. Elser, D.S. Gruner, H. Hillebrand, J.B. Shurin, J.E. Smith. *Nutrient co-limitation of primary producer communities.* Ecol. Lett., 125 (2011), 852–862.

[12] S.-B. Hsu, K.-S. Cheng, S.P. Hubbell. *Exploitative competition of microorganisms for two complementary nutrients in continuous cultures.* SIAM J. Appl. Math., 41:3 (1981), 422–444 .

[13] J. Huisman, F.J. Weissing. *Biological conditions for oscillations and chaos generated by multispecies competition.* Ecology, 82:10 (2001), 2682–2695 .

[14] G. E. Hutchinson. *The paradox of the plankton.* Am. Nat., 95:882 (1961), 137–145.

[15] B.W. Kooi, M.P. Boer, S.A.L.M. Kooijman. *Resistance of a food chain to invasion by a top predator.* Math. Biosci., 157 (1999), 217–236.

[16] B.W. Kooi. *Numerical bifurcation analysis of ecosystems in a spatially homogeneous environment.* Acta Biotheor., 51:3 (2003), 189–222,.

[17] B.W. Kooi, L.D.J. Kuijper, S.A.L.M. Kooijman. *Consequence of symbiosis for food web dynamics.* J. Math. Biol., 49:3 (2004), 227–271.

[18] S.A.L.M. Kooijman. *Dynamic Energy Budget theory for metabolic organisation.* Cambridge University Press, Cambridge, 2010.

[19] S.A.L.M. Kooijman, H.A. Dijkstra, B.W. Kooi. *Light-induced mass turnover in a mono-species community of mixotrophs.* J. Theor. Biol., 214 (2002), 233–254.

[20] Yu.A. Kuznetsov. *Elements of Applied Bifurcation Theory.* volume 112 of Applied Mathematical Sciences. Springer-Verlag, New York, 3 edition, 2004.

[21] T.E. Miller, J.H. Burns, P. Munguia, E.L. Walters, J.M. Kneitel, P. M. Richards, N. Mouquet, H. L. Buckley. *A critical review of Twenty Years' use of the Resource-Ratio Theory*. Am. Nat., 165:4 (2005), 439–448.

[22] R.D. Morton, R. Law, S.L. Pimm, J.A. Drake. *On models for assembling ecological communities*. Oikos, 75:3 (1996), 493–499 .

[23] S. Nattrass, S. Baigent, D.J. Murrell. *Quantifying the likelihood of co-existence for communities with asymmetric competition*. B. Math. Biol., 74:10 (2012), 2315–2338.

[24] R.V. O'Neill, D.L. DeAngelis, J.J. Pastor, B.J. Jackson, W.M. Post. *Multiple nutrient limitations in ecological models*. Ecol. Model., 46 (1989), 147–163.

[25] P. Schipper, A.M. Verschoor, M. Vos, W.M. Mooij. *Does "supersaturated coexistence" resolve the "paradox of the plankton"?* Ecol. Lett., 4 (2001), 404–407.

[26] E. Sperfeld, D. Martin-Creuzburg, A. Wacker. *Multiple resource limitation theory applied to herbivorous consumers: Liebig's minimum rule vs. interactive co-limitation*. Ecol. Lett., 15 (2012) 142–150.

[27] H.L. Smith, P. Waltman. *The Theory of the Chemostat.* Cambridge University Press, Cambridge, 1994.

[28] T.A. Troost, B.W. Kooi, S.A.L.M. Kooijman. *Bifurcation analysis can unify ecological and evolutionary aspects of ecosystems*. Ecol. Model., 204 (2007), 253-268.

[29] D. Tilman. *Resource competition between planktonic algae: an experimental and theoretical approach*. Ecology, 58 (1977), 338–348.

[30] D. Tilman. *Resources: A graphical-mechanistic approach to competition and predation*. Am. Nat., 116 (1980), 363–393.

[31] D. Tilman. *Resource competition and community structure.* Princeton University Press, Princeton, 1982.

[32] D. Tilman. *The resource-ratio hypothesis of plant succession*. Am. Nat., 125:6 (1985), 827–852.

[33] D. Tilman. *Plant strategies and the Dynamics and Structure of Plant Communities*. Princeton University Press, Princeton, 1988.

[34] J.B. Wilson, E. Spijkerman, J. Huisman. *Is there really insufficient support for Tilman's R^* concept? A comment on Miller et al.*. Am. Nat., 169:5 (2007), 700–706.